RSC Advances

PAPER

View Article Online
View Journal | View Issue

Cite this: *RSC Adv.*, 2025, **15**, 30436

Photochemical reaction of 4-chlorobiphenyl with nitrous acid in atmospheric aqueous solution

Yue Yang, [abc] Yadong Hu,[abc] Wenli Liu,[abc] Hui Cai,[abc] Chengzhu Zhu *[abc] and Mingjin Wang*[abc]

The photochemical reaction of 4-chlorobiphenyl (4-PCB) and HONO in atmospheric aqueous phase was studied by 355 nm laser flash photolysis combined with 365 nm UV steady-state irradiation technique. The steady-state study showed that the conversion rate of 4-PCB was affected by the initial concentration of 4-PCB, pH value and HONO concentration, while chloride ions had little effect on the conversion of 4-PCB. HONO produces an HO˙ attack on 4-PCB to form a 4-PCB-OH adduct with the second-order reaction rate constant of $(9.0 \pm 1) \times 10^9$ L mol^{-1} s^{-1}. The 4-PCB-OH adduct continues to react with HONO and O_2 with second-order rate constants of $(5.3 \pm 0.1) \times 10^6$ L mol^{-1} s^{-1} and $(4.9 \pm 0.2) \times 10^6$ L mol^{-1} s^{-1}, respectively. The main transient intermediates of 4-PCB-OH adducts had a variety of decay pathways, and the final products mainly included 4-hydroxybiphenyl, 4-chlorobenzyl-4-ol, 4-chlorobenzyl-4-nitrobiphenyl, and 4-(4-chlorophenyl-2-nitrophenol). The formation mechanism of these products was also discussed.

Received 6th April 2025
Accepted 17th August 2025

DOI: 10.1039/d5ra02373d

rsc.li/rsc-advances

1. Introduction

Nitrous acid (HONO) is an important pollutant in the troposphere and is widely distributed in the atmosphere,[1–3] due to its high Henry's coefficient (49 mol L^{-1} atm^{-1}), it could quickly dissolve into atmospheric liquid such as rain, fog, clouds or wet aerosols.[4] At present, the measured concentration of nitrite is between 10^{-7}–10^{-6} mol L^{-1} in atmospheric liquid such as clouds and nectar water.[5]

The role of nitrous acid (HONO) in atmospheric chemistry has received considerable attention in recent years.[6] Sources of HONO include (a) direct emission (*e.g.*, vehicle exhaust, soil emission, livestock manure, and biomass burning),[7] (b) the homogeneous reaction of NO and ˙OH,[8,9] (c) the heterogeneous reaction of NO_2 on aerosol surface and ground (dark and photosensitized reactions),[10] and (d) the photolysis of nitrate.[11] Heterogeneous reactions are widely recognized as the major sources of HONO.[12] Liu *et al.*[13] found that the multiphase reaction of NO_2 at the aerosol surface and ground surface might be responsible for 40% and 36% of HONO production from 2017 to 2018 in Nanjing, respectively. Besides urban areas, Xue *et al.*[14] found that NO_2 uptake onto ground surface dominated (~70%) the nighttime HONO formation while the photo-enhanced heterogeneous reaction dominated (~80%) daytime HONO formation at Mt. Tai in summer 2018. The UV photolysis of HONO was a major source of HO˙ accounting for 20–90%,[15–17] in the troposphere during the early morning and in indoor environments, which triggers the oxidation of many atmospheric species, leading to the formation of ozone (O_3) and secondary aerosol.[17–19]

$$\mathrm{HONO} + h\nu \rightarrow \mathrm{HO}^{\bullet} + \mathrm{NO}^{\bullet} \quad (320\ \mathrm{nm} < \lambda < 400\ \mathrm{nm}) \qquad (1)$$

Polychlorinated biphenyls (PCBs), containing 209 individual compounds (so-called congeners), had been of global concern as persistent organic pollutants listed by the Stockholm convention.[20–22] PCBs could cause a variety of adverse effects due to their bio-accumulation, environmental persistence, and high toxicity.[23–25] PCBs can spread to remote areas such as polar region through atmospheric circulation, ocean currents, *etc.* Studies have shown that PCBs have been detected in marine organisms and indigenous peoples in the Arctic region, confirming their global pollution characteristics. Under normal conditions, most PCBs were colorless and crystalline, and only a few of PCBs with fewer Cl atoms exist in liquid form.[26] PCBs were mostly used as heat conduction liquids in electronic devices such as capacitors or transformers because of their flame-retardant hydrophobic, hydrolytic and oxidation resistance.[27] Chen *et al.*[28] reported the total concentration of PCBs in the atmosphere and particulate matter in a typical PCBs pollution area in Zhejiang Province was 191–641 ng m^{-3} and 191–373 ng g^{-1}. PCBs mainly existed in the atmosphere as molecules, adsorbed on particulate matter or dissolved in atmospheric droplets.[29] Hong *et al.*[30] measured that the concentration of PCBs in the atmosphere of Beijing was about

[a]*School of Resource and Environmental Engineering, Hefei University of Technology, Hefei 230009, P.R. China. E-mail: czzhu@hfut.edu.cn; wangmingjin@vip.163.com; Fax: +86 551 62901649; Tel: +86 551 62901523*

[b]*Institute of Atmospheric Environment & Pollution Control, Hefei University of Technology, Hefei 230009, P.R. China*

[c]*Key Laboratory of Nanominerals and Pollution Control of Anhui Higher Education Institutes, Hefei University of Technology, Hefei 230009, P.R. China*

8.42–45.2 ng m^{-3}. At present, the methods of treating PCBs were mainly divided into physical remediation (deep burial, transfer, thermal desorption and solvent leaching, *etc.*), chemical remediation (incineration and non-incineration) and biological remediation (mainly plant and microbial remediation),[31] while the photochemical processes of PCBs in atmosphere were rarely reported.

Wu *et al.*[32] found OH radical would attack PCB-209 to form hydroxyl substitution products, with the release of chlorine and pentachlorobenzene radicals. Extensive scientific studies confirmed that nitrogen dioxide (NO_2) played a crucial role in atmospheric nitration processes in both gas and liquid phases, whereas the specific mechanism of nitrous acid (HONO) in atmospheric aqueous-phase nitration remained unclear.[33] The present work selected 4-chlorobiphenyl (4-PCB) as a model compound to investigate the photochemical reaction with HONO and its influence in atmospheric aqueous solution. The effects of various factors on 4-PCB photo-conversion were evaluated by 365 nm UV light irradiation steady-state experiments. The reaction rate of 4-PCB with $HO^{\bullet}$ was determined by 355 nm laser flash photolysis[34] and the decay of intermediates was discussed. The transformation products were identified by GC-MS, and its possible reaction pathway was elucidated.

2. Materials and methods

2.1 Chemicals and reagents

4-Chlorobiphenyl and $NaNO_2$ (99.0%, Shanghai Chemical Reagents Co., China) were used as received. HONO was prepared by acidifying the corresponding $NaNO_2$ solution to a pH value of approximately 1.5 to make NO_2 existed in the form of HONO. The pH values of the sample solutions were adjusted using $HClO_4$. The oxygenation or deoxygenating of the sample solutions was achieved by bubbling high-purity oxygen (99.5%) or nitrogen (99.999%) for 30 min. All chemicals were of analytical grade, and all experiments were performed at 25 ± 2 °C.

2.2 Irradiation experiments

In a 200 mL cylindrical quartz reactor, aqueous solution of 4-PCB and HONO was prepared, and to ensure that there was no other gas interference in the mixed solution, and constantly bubbled with high-purity N_2 or O_2 to keep the pure atmosphere for 15 min. UV lamps would be covered with waterproof quartz spacers (8 W, 365 nm) was placed in the middle of the reactor, so that the mixed solution was uniformly irradiated (irradiation intensity was 1.5 mW cm^{-2}). In order to ensure that the solution was evenly mixed under illumination, a magnetic agitator was placed below the quartz apparatus, and a magnetic rotor was placed at the bottom of the quartz apparatus. $HClO_4$ was used to adjust the pH value of the reaction solution.

2.3 Laser flash photolysis

In this study, a laser flash photolysis spectrometer (LP920, Edinburgh Instrument, UK) was used to record nanosecond level transient absorption spectra and kinetic signals of samples. Laser conditions were as follows: wavelength was 355 nm, pulse width was 4–6 ns, energy was 30 ± 5 mJ $pulse^{-1}$, and laser spot radius was 0.3 cm. The details and schematic diagram of the LFP spectrometer had been described in our previous reports.[35]

2.4 Analytical methods

The concentration of 4-PCB was determined by a high-performance liquid chromatography (HPLC, Dionex UltiMate 3000) with the following conditions: with a Thermo C18 column (5.0 μm, 4.6 mm × 150 mm) at a detection wavelength of 254 nm. The mobile phase consisted of 90% methanol and 10% water, where the flow rate was set at 1.0 mL min^{-1}. The column oven temperature was 30 °C, and the injection volume was 20.0 μL.

The UV-vis absorbance spectrum was recorded by using Shimadzu UV1750. A dissolved oxygen meter (SX825, Shanghai San-Xin Instrumentation Inc. China) was used to measure the concentration of dissolved oxygen in the solution.

GC-MS (Agilent 7890A–5975C, America) was used to identify the photoproducts of 4-PCB transformation. GC-MS with the following conditions: HP-5MS capillary column (30 m × 0.25 mm, 0.25 μm diameter) for gas chromatographic separation with helium as carrier gas, with a flow rate 1.0 mL min, an injection volume 1 μL, and an injection port temperature of 280 °C. Temperature programming: the initial temperature was 50 °C for 5 min, and the speed was 5 °C min^{-1}, which was increased to 250 °C and kept for 15 min and the EI ion source was used at 230 °C for detection.

3. Results and discussion

3.1 Steady-state studies

3.1.1 UV-vis absorption of 4-PCB and HONO solution. The UV-vis absorption spectra of 7×10^{-5} mol per L 4-PCB (pH = 6.7) and 5×10^{-3} mol per L HONO (pH = 2.87) were shown in Fig. 1. The absorption bands for HONO exhibited strong absorption between 300–400 nm, suggesting HONO could be excited by 355 nm or 365 nm irradiation, whereas 4-PCB were not more than 300 nm and the maximum absorption peak height was about 250 nm, indicating it could not be excited.

3.1.2 Effects of 4-PCB initial concentration. The influence of different concentrations of 4-PCB on the conversion and transformation of 4-PCB at pH 1.5 was shown in Fig. 2a. The conversion process of 4-PCB obeyed pseudo-first-order kinetics, so the rate expression of the reaction between *o*-DCB and HONO could be written as:

$$\frac{d[\text{4-PCB}]}{dt} = -k_{obs}[\text{4-PCB}][\text{HONO}] \quad (2)$$

where [4-PCB] and [HONO] were the concentrations of 4-PCB and HONO, respectively. k_{obs} was the observed conversion rate of 4-PCB.

With the initial concentration of 4-PCB increased from 1×10^{-5} mol L^{-1} to 7×10^{-5} mol L^{-1}, its decay rate decreased from 0.043 min^{-1} to 0.019 min^{-1}. The decay constant of 4-PCB decreased with increasing initial concentration of 4-PCB. This

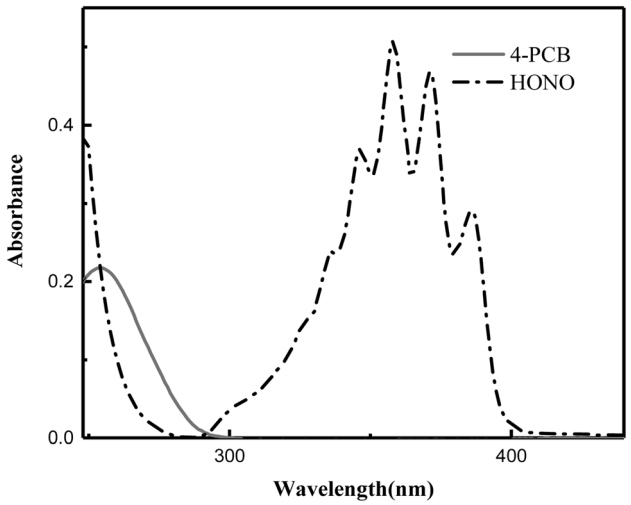

Fig. 1 UV-vis absorption spectra of 4-PCB and HONO solution.

was similar to the results of Ma *et al.*, who used UV to degrade biphenyl.[36] As the concentration of 4-PCB increased, the transmission of UV rays was reduced and more by-products were produced, the steady-state concentration of HO˙ was reduced, resulting in a lower quasi-primary conversion rate of the target compound.

3.1.3 Effects of HONO concentration. In the solution containing 7×10^{-5} mol per L 4-PCB (pH = 1.5), the influence of the change of initial HONO concentration on the conversion and transformation of 4-PCB was investigated in Fig. 2b, the conversion rate of 4-PCB increased from 0.00845 min^{-1} to 0.02203 min^{-1} as the concentration of HONO increased from 1×10^{-3} mol L^{-1} to 7.5×10^{-3} mol L^{-1}. The increase of HONO concentration led to the enhancement of HO˙ generation, which accelerated the conversion of 4-PCB. However, when the concentration of HONO exceed 7×10^{-3} mol L^{-1}, the conversion rate of 4-PCB basically remained unchanged. Because other reactions occurred in the solution:[35]

$$HONO + HO^{\cdot} \rightarrow H_2O + {}^{\cdot}NO_2 \quad k = 1 \times 10^9\ L\ mol^{-1}\ s^{-1} \quad (3)$$

$$NO_2^- + HO^{\cdot} \rightarrow OH^- + NO_2 \quad k = 1 \times 10^{10}\ L\ mol^{-1}\ s^{-1} \quad (4)$$

When the concentration of HONO continued to increase, the collision probability between free radical increased, and the reaction between HO˙ and HONO and NO_2^- consumed a lot of

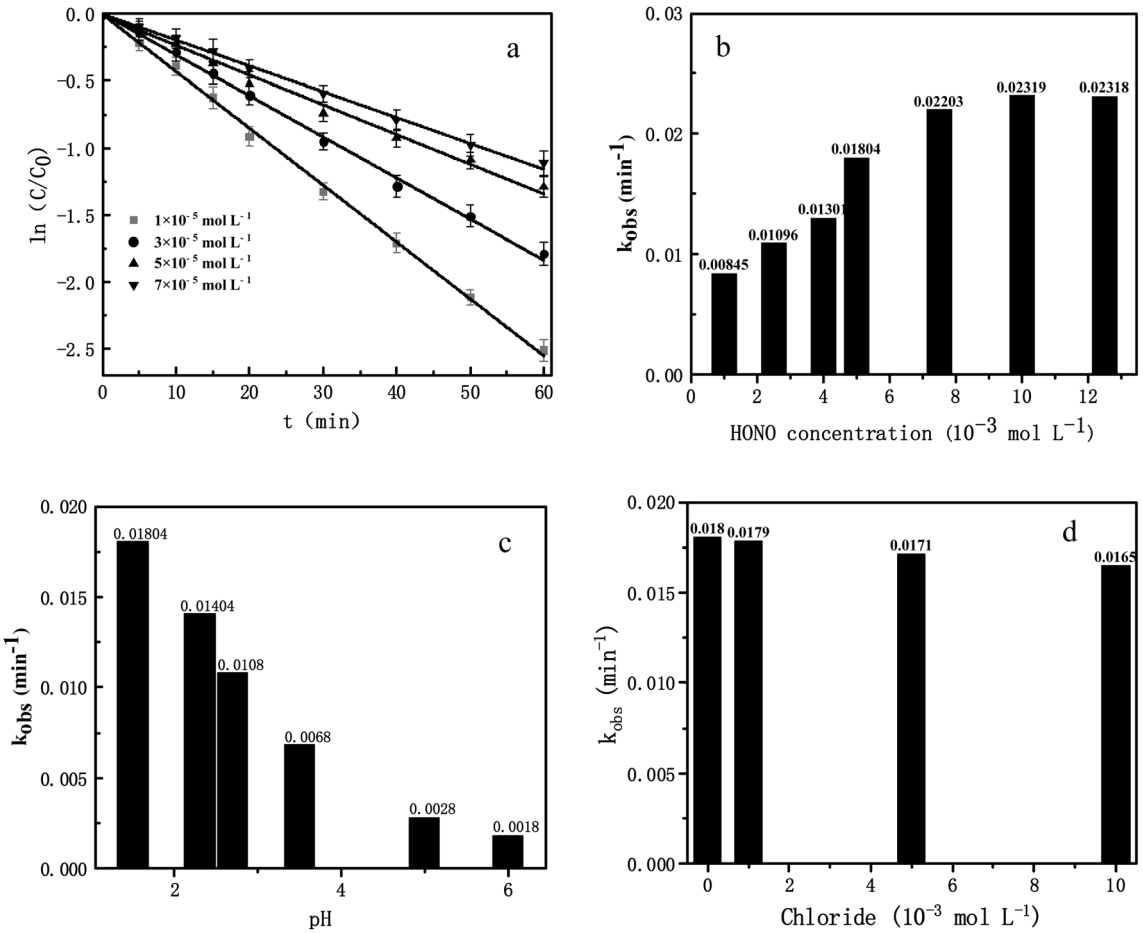

Fig. 2 (a) The effect of initial 4-PCB concentration on 4-PCB degradation. (b) The effect of initial HONO concentration on 4-PCB degradation. (c) The effect of pH on 4-PCB degradation. (d) The effect of chloride on 4-PCB degradation.

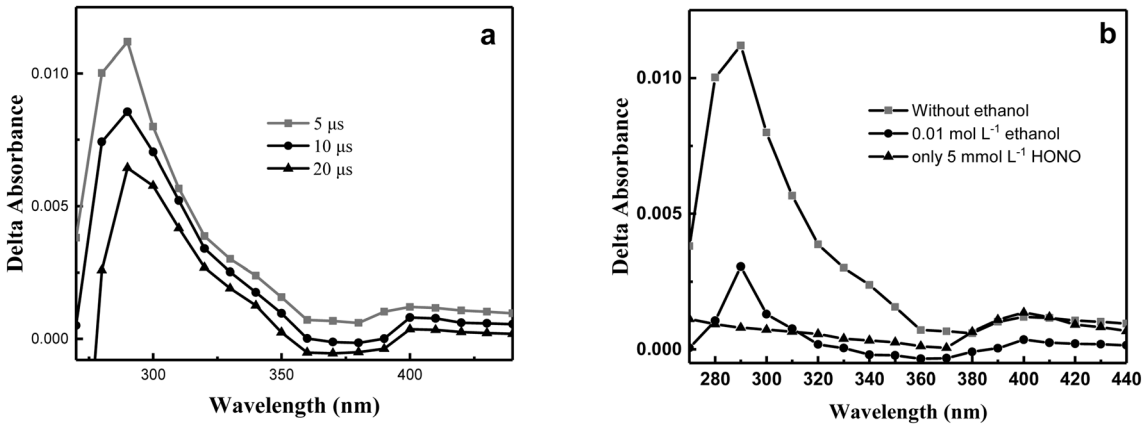

Fig. 3 (a) Transient absorption spectrum of a mixed solution of HONO and 4-PCB in N_2 atmosphere after 355 nm laser excitation. (b) With ethanol.

HO•, when the concentration of HONO exceed the optimum concentration, the increase of HONO concentration would inhibit the conversion process of 4-PCB. It was similar to the research results of Ma *et al.*,[36] who believed that when the concentration of HONO was too high, the HO• would react with HONO and NO_2^-, thus inhibiting the collision between pollutants and HO•.

3.1.4 Effects of initial pH value. Due to pH of the atmospheric liquid phase was between 1.95 and 7.74,[37] the pH value range of 1.5 to 6.0 was selected to explore the effect of pH value on 4-PCB conversion in this experiment. It was found that the conversion rate of 4-PCB decreased with increasing pH value from 1.5 to 6 in Fig. 2c. The low pH would promote the content of HONO to be higher, while high pH would promote the conversion of HONO to NO_2^-.[33] However, HONO had higher HO• quantum yield than NO_2^-.[38] Therefore, higher pH would make the content of HO• insufficient and limit the conversion of 4-PCB.

3.1.5 Effects of Cl^-. There were many soluble halogen ions in the atmospheric liquid phase.[39] In the real atmospheric environment, the specific situation of chloride ions to HO• induced 4-PCB conversion process still had many deficiencies.

$$HO^\bullet + Cl^- \rightarrow ClOH^- \quad k = 4.3 \times 10^9\ L\ mol^{-1}\ s^{-1} \qquad (5)$$

The chloride ions competed to consume the HO•, and the rate constant of OH radical with chloride ions was 4.3×10^9 L mol^{-1} s^{-1}.[36] HO• also interacted with chloride ions to generate some active chlorine free radicals, which might participate in the 4-PCB conversion process. As shown in Fig. 2d, Cl^- concentration from 1×10^{-3} mol L^{-1} to 1×10^{-2} mol L^{-1} had little effect on the conversion of 4-PCB.

3.2 Laser flash photolysis studies

3.2.1 Time-resolved transient absorption spectra of N_2-saturated HONO and 4-PCB mixed solutions. Under the condition of pH 1.5, the N_2 saturated mixed solution containing 5×10^{-3} mol per L HONO and 7×10^{-5} mol per L 4-PCB was subjected to laser flash photolysis at 355 nm, and two transient absorption bands of about 260–360 nm and 400 nm were

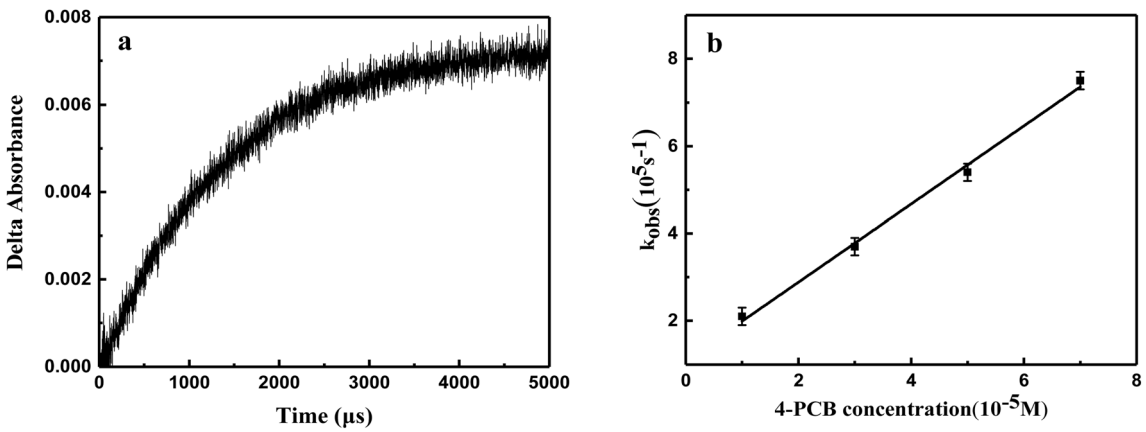

Fig. 4 (a) Net growth curve of transient material at 290 nm. (b) The linear relationship between the pseudo-first-order transient generation rate at 290 nm and different 4-PCB concentrations. The second-order rate constant deriving from the slope of straight line was $(8.9 \pm 0.2) \times 10^9$ L mol^{-1} s^{-1}.

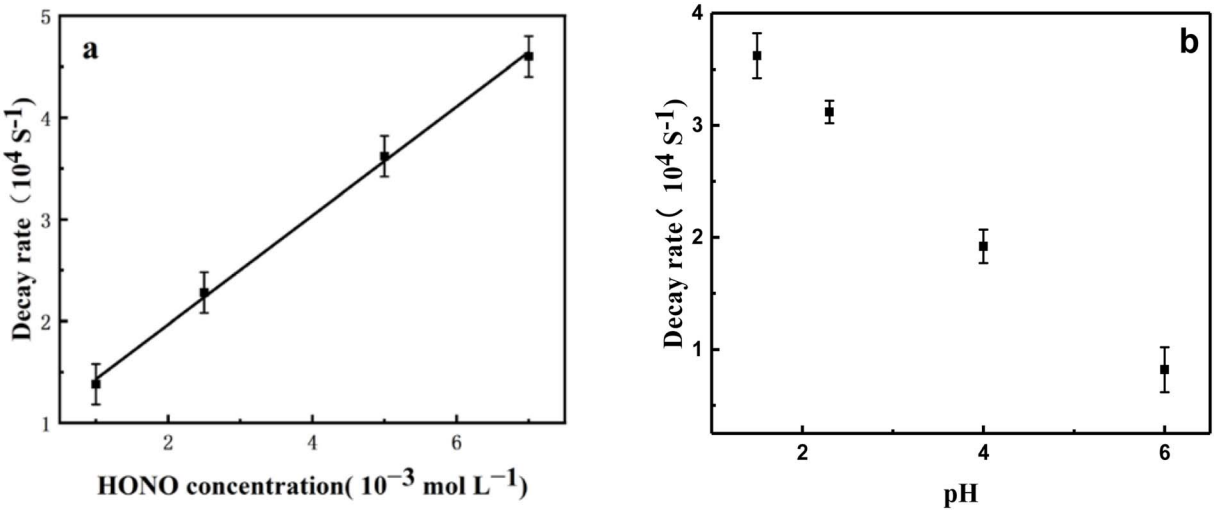

Fig. 5 (a) Effect of HONO concentration on the decay rate of 4-PCB-OH adducts. The second-order rate constant deriving from the slope of straight line was (5.3 ± 0.1) × 10^6 L mol^{-1} s^{-1}. (b) Effect of pH value on the decay rate of 4-PCB-OH adducts at a HONO concentration of 5 × 10^{-3} mol L^{-1}.

observed (Fig. 3a). Ethanol was considered as an effective HO˙ quencher.[40] When ethanol was added, the two transient bands of 260–360 nm and 390–410 nm were greatly reduced (Fig. 3b), indicating that the transient substances in these two transient bands were related to HO˙. The peak absorption in the range of 260–360 nm represents the characteristic absorption peaks of hydroxycyclohexadienyl radicals, which were generated from the addition of HO˙ on the aromatic ring.[41] Therefore, the absorption spectra in the range of 260–360 nm were assigned to the 4-PCB-OH adducts generated from the following reaction:[42]

$$\text{4-PCB} + \text{HO}^{\cdot} \rightarrow \text{4-PCB-OH adduct} \quad (6)$$

The kinetic study showed that the formation of 4-PCB-OH adduct at 290 nm obeyed the pseudo-first-order reaction kinetics, and the $k_{growth} = 7.5 \times 10^5$ s^{-1} (Fig. 4a). According to the linear relationship between the first-order growth rate constant and the concentration of DMP, the second-order reaction rate constant of the reaction between HO˙ and 4-PCB was determined to be (8.9 ± 0.2) × 10^9 L mol^{-1} s^{-1} (Fig. 4b), which was consistent with the result reported by Sehested *et al.*[43] with the second-order reaction rate of HO˙ and biphenyl was (9.0 ± 1) × 10^9 L mol^{-1} s^{-1}.

The dynamics of 400 nm transient species showed that growth and decay obey the rule of pseudo-first-order kinetics reaction. The results were completely different from those observed at 310 nm, indicating that the transient substance was not a 4-PCB-OH adduct. The photodegradation results of HONO were compared with the transient kinetic parameters, and it was found that the absorption peak height was similar at 400 nm.

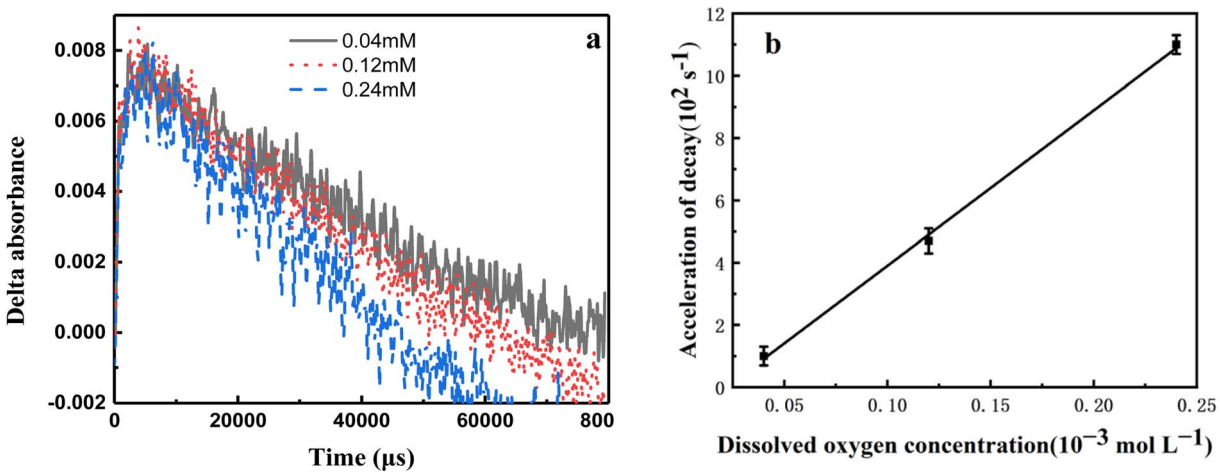

Fig. 6 (a) Kinetic curve of 4-PCB-OH adduct under different dissolved oxygen concentration. (b) The accelerated effect of dissolved oxygen concentration on the pseudo-first-order degradation rate of 4-PCB-OH adducts. The second-order rate constant deriving from the slope of straight line was (4.9 ± 0.2) × 10^6 L mol^{-1} s^{-1}.

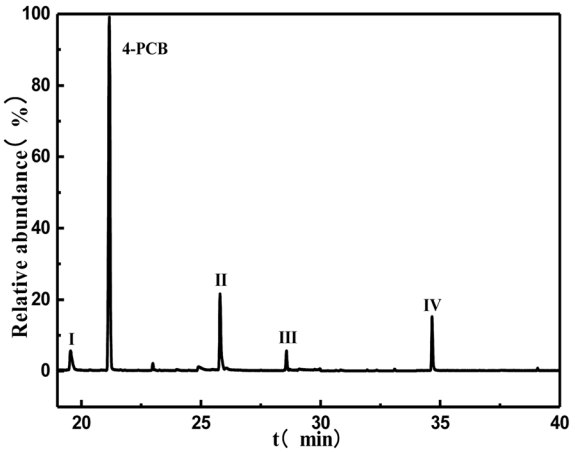

Fig. 7 The TIC of the reaction sample after illumination at 365 nm.

Transient species at 400 nm were attributed to $NO_2^{\bullet}$, according to previous literature.[35,36]

3.3 Decay kinetics of 4-PCB-OH adducts

HONO was highly oxidizing, Zhu *et al.*[44] found nitrobenzene in the product. When studying the reaction mechanism of 4.2×10^{-4} mol per L benzene and 5×10^{-3} mol per L HONO (pH = 1.5). They believed that nitrobenzene was produced due to the nitration of benzene-OH adducts by HONO. In the solution containing 7×10^{-5} mol per L 4-PCB (pH = 1.5), with HONO concentration increasing from 1×10^{-3} mol L^{-1} to 7×10^{-3} mol L^{-1}, 4-PCB-OH adducts, the first-order decay rate constant of the adducts increased from 1.38×10^4 to 4.6×10^4 s^{-1} in Fig. 5a, indicating that the decay rate of 4-PCB-OH adducts could be accelerated by HONO. By establishing the curve of 4-PCB-OH decay rate relative to HONO concentration, the second order reaction rate constant of 4-PCB-OH adduction and HONO was determined to be $(5.3 \pm 0.1) \times 10^6$ L mol^{-1} s^{-1}. As mentioned above, at low pH, the dissociation equilibrium shifts towards HONO production, and HONO had a higher HO$^{\bullet}$ quantum yield. The 4-PCB-OH adduct had a faster decay rate at low pH in Fig. 5b, thus the reaction with HO$^{\bullet}$ was also an important decay pathway of 4-PCB-OH adduct.

The effect of oxygen on the decay of 4-PCB-OH adducts was also investigated because of the abundant dissolved oxygen in atmospheric droplets. In Fig. 6a, the decay rate of the transient substance at 310 nm increased as the concentration of dissolved oxygen increased from 4×10^{-5} mol L^{-1} to 2.4×10^{-4} mol L^{-1} (from 1×10^{-2} s^{-1} to 11×10^{-2} s^{-1}). The results showed that the 4-PCB-OH adduct could react with oxygen molecules. By fitting the linear relationship of the influence of the increase of dissolved oxygen concentration on the decay rate of 4-PCB-OH adduction, it could be concluded that the second-order reaction rate constant of 4-PCB-OH adduction with O_2 was $(4.9 \pm 0.2) \times 10^6$ L mol^{-1} s^{-1} in Fig. 6b. This value was close to the second-order reaction rate constant of 2-PCB-OH adduction with O_2 reported by Huang *et al.*[45] which was $(5.4 \pm 0.2) \times 10^6$ L mol^{-1} s^{-1}.

3.4 Products analysis

In order to further understand the mechanism of photochemical reaction between 4-PCB and HONO, the conversion products were identified by GC-MS. After irradiated 100 mL N_2 saturated mixed solution containing 7×10^{-5} mol per L 4-PCB and 5×10^{-3} mol per L HONO (pH = 1.5) with 365 nm ultraviolet light for 30 min, sample was extracted with CH_2Cl_2 for 3 times, and the extracted organic phase was dried with anhydrous sodium sulfate for 12 h, and then concentrated to 1.5 mL with rotary evaporator.

The mass spectra corresponding to each peak in Fig. 7 were compared with the NIST standard mass spectrometry library to identify the product types including 4-hydroxybiphenyl, 4-chlorophenyl-4-ol, 4-chlorophenyl-4-nitrobiphenyl and 4-(4-chlorophenyl-2-nitrophenol), respectively.

Fig. 8 showed the derivation of the reaction mechanism between HONO and 4-PCB under the irradiation of 365 nm UV lamp. Hizal *et al.*[46] and Ma *et al.*[47] found that the addition of HO$^{\bullet}$ on the aromatic ring would cause the bond breaking. HO$^{\bullet}$

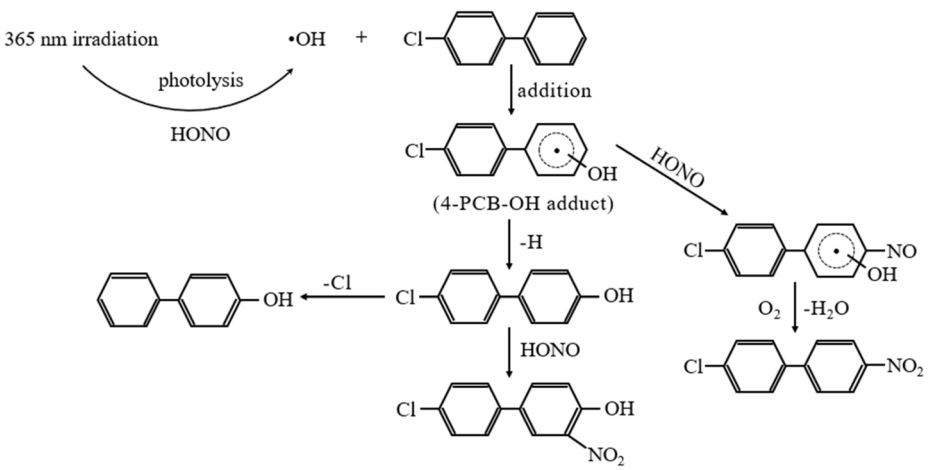

Fig. 8 The proposed reaction mechanisms of 4-PCB with HONO under 365 nm irradiation.

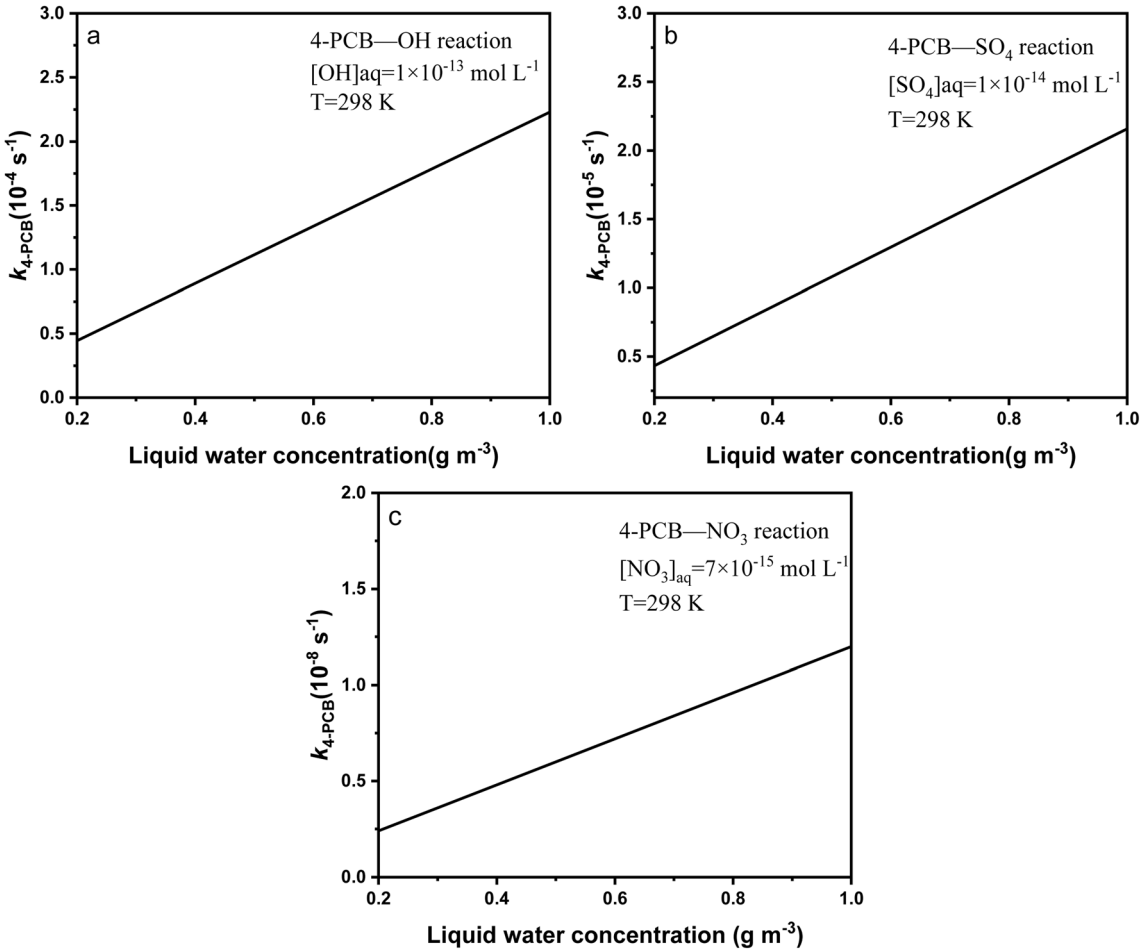

Fig. 9 Oxidation rate of 4-PCB in atmospheric liquid phase reacted with different free radicals. (a) $^{\bullet}OH$, (b) $SO_4^{-\bullet}$ and (c) $NO_3^{\bullet}$.

produced by photolysis of HONO would attack the benzene ring of chlorobenzene to form a 4-PCB-OH admixture. Due to the electron absorption effect of chlorine atom, the electron cloud density of the benzene ring replaced by chlorine atom would be reduced, $HO^{\bullet}$ was more likely to be added to the benzene ring not replaced by chlorine atom.[48] Therefore, it was dehydrogenated to form 4-chlorophenyl-4-alcohol. Cao *et al.*[49] found that reported that when PCBS was degraded, the hydroxylation reaction of PCBs released chloride ions, leading to the formation of 4-hydroxybiphenyls. Therefore, the 4-hydroxybiphenyls might be formed by the cleavage of the C–Cl bond after the addition of $HO^{\bullet}$ to the benzene ring. In Fig. 7, the 4-hydroxybiphenyls were produced in small quantities.

$$\text{4-PCB} + HO^{\bullet} \rightarrow \text{4-PCB-OH} \quad (7)$$

$$\text{4-PCB-OH} + \text{HONO} \rightarrow \text{4-PCB-OH-NO}_2 + H_2 \quad (8)$$

As mentioned above, HONO also played an irreplaceable role in the nitrification process in the liquid phase of the atmosphere. Huang *et al.*[45] also detected nitrochlorobenzene in the photochemical experiments on 2-chlorobenzene and HONO. This research bore out the idea that it was caused by the interaction of 2-chlorobenzene cationic radicals with nitrous acid. Therefore, the generation of 4-chloro-4′-nitrobiphenyl in this experiment was generated by the interaction of 4-chlorobiphenyl cationic radical with nitrite. Fischer and Warneck[50] found in the study of the photochemical reaction between benzene and HONO that phenol, the product of benzene's reaction with $HO^{\bullet}$ in the photolysis process of HONO, would be nitrated by HONO to produce nitrophenol. Thus, 4-(4-chlorophenyl)-2-nitrophenol could be produced by nitration of 4-chlorophenyl-4-ol by HONO (formed by eqn (8)).[42]

3.5 Atmospheric implication

In the troposphere, long-wavelength radiation could not directly excite 4-PCB, it primarily undergoes indirect phototransformation *via* radical-induced reactions, while the role of highly reactive radicals such as $^{\bullet}OH$, $^{\bullet}SO_4$ and $^{\bullet}NO_3$ radicals could be considerable. Assuming that the air–water interface *etc* heterogeneous reactions was not considered, the oxidation rate constant of 4-PCB reacted with reactive radicals in the liquid phase could be theoretically calculated as:[51]

$$k_{\text{4-PCB-OH}} = k_{OH^{\bullet}}[OH^{\bullet}]_{aq} LRT \quad (9)$$

$$k_{4\text{-PCB-}SO_4^{-\cdot}} = k_{SO_4^{-\cdot}}[SO_4^{-\cdot}]_{aq} LRT \quad (10)$$

$$k_{4-PCB-NO_3^{\cdot}} = k_{NO_3^{\cdot}}[NO_3^{\cdot}]_{aq} LRT \quad (11)$$

where k_{OH} was the reaction constant of 4-PCB with the $OH^{\cdot}$ radical and was measured to be 9.0×10^9 L mol^{-1} s^{-1} in this work; $k_{SO_4^{-\cdot}}$ was the reaction rate constant of 4-PCB with $SO_4^{-\cdot}$ and was 8.7×10^9 L mol^{-1} s^{-1}; $k_{NO_3^{\cdot}}$ was the reaction rate constant of 4-PCB with $NO_3^{\cdot}$ and was 6.9×10^9 L mol^{-1} s^{-1}; L was the liquid water concentration (g m^{-3}); R was the thermodynamic constant, which was 8.314 J mol^{-1} K^{-1}; and T was the thermodynamic temperature (K).[52,53] $[OH^{\cdot}]_{aq}$ was the concentration of $OH^{\cdot}$ radicals in liquid water such as clouds, and $OH^{\cdot}$ radical concentration 1×10^{-13} mol L^{-1} in atmosphere.[54,55] $[NO_3^{\cdot}]_{aq}$ was the concentration of $NO_3^{\cdot}$ radical in the liquid phase of the atmosphere, and $NO_3^{\cdot}$ radical concentration was 7.0×10^{-15} mol L^{-1}. $SO_4^{-\cdot}$ radical concentration was 1.0×10^{-14} mol L^{-1} in the liquid phase.

The oxidation rates of OH radical (Fig. 9), $NO_3^{\cdot}$ radical and $SO_4^{-\cdot}$ radical with 4-PCB were estimated 4.46×10^{-5}–2.23×10^{-4} s^{-1}, 2.4×10^{-9}–1.2×10^{-8} s^{-1}, 4.32×10^{-6}–2.16×10^{-5} s^{-1}, respectively. The corresponding lifetime were 0.26–0.05 days, 4822–964.5 days, and 2.68–0.53 days, respectively. It indicated OH radical played a leading role in the atmospheric oxidation of 4-PCB.

4. Conclusions

The photochemical reaction kinetics and mechanisms between 4-PCB and HONO in the aqueous solution were investigated. The results showed that HONO produces $HO^{\cdot}$ attacking 4-PCB to form 4-PCB-OH adduction, and its second-order rate constant was $(9.0 \pm 1) \times 10^9$ L mol^{-1} s^{-1}. Then, the 4-PCB-OH adjuncts continue to react with HO, NO and O_2, and the second-order rate constants were $(5.3 \pm 0.1) \times 10^6$ L mol^{-1} s^{-1} and $(4.9 \pm 0.2) \times 10^6$ L mol^{-1} s^{-1}, respectively. The main transient intermediates, 4-PCB-OH adjuncts, had a variety of decay pathways and were eventually converted into stable products including 4-hydroxybiphenyls, 4-chlorophenyl-4-alcohols, 4-chloro-4′-nitrobiphenyls, and 4-(4-chlorophenyl)-2-nitrophenol. The atmospheric model indicated OH radical played a leading role in the atmospheric oxidation of 4-PCB.

Author contributions

Yue Yang: investigation, conceptualization, formal analysis, data curation, writing – original draft. Yadong Hu: investigation, methodology, validation, formal analysis. Wenli Liu: investigation, validation. Hui Cai: investigation, formal analysis. Chengzhu Zhu: supervision, methodology, conceptualization, validation, resources, funding acquisition, project administration, writing – review & editing. Mingjin Wang: methodology, resources.

Conflicts of interest

The authors declared that they had no conflicts of interest to this work.

Data availability

The data included in the manuscript.

Acknowledgements

The authors thank for the financial support from National Natural Science Foundation of China (NSFC) (22376049 and 21876038) for support this study.

References

1 L. Sun, T. S. Chen, Y. Jiang, Y. Zhou, L. F. Sheng, J. T. Lin, J. Li, C. Dong, C. Wang, X. F. Wang, Q. Z. Zhang, W. X. Wang and L. K. Xue, Ship emission of nitrous acid (HONO) and its impacts on the marine atmospheric oxidation chemistry, *Sci. Total Environ.*, 2020, **735**, 139355, DOI: 10.1016/j.scitotenv.2020.139355.

2 P. V. Pawar, A. S. Mahajan and S. D. Ghude, HONO chemistry and its impact on the atmospheric oxidizing capacity over the Indo-Gangetic Plain, *Sci. Total Environ.*, 2024, **947**, 174604, DOI: 10.1016/j.scitotenv.2024.174604.

3 X. R. Zhang, S. R. Tong, C. H. Jia, W. Q. Zhang, Z. Wang, G. Q. Tang, B. Hu, Z. R. Liu, L. L. Wang, P. S. Zhao, Y. P. Pan and M. F. Ge, Elucidating HONO formation mechanism and its essential contribution to OH during haze events, *npj Clim. Atmos. Sci.*, 2023, **6**, 55, DOI: 10.1038/s41612-023-00371-w.

4 Y. He, X. L. Zhou, J. Hou, H. L. Gao and S. B. Bertman, Importance of dew in controlling the air-surface exchange of HONO in rural forested environments, *Geophys. Res. Lett.*, 2006, **33**, L02813, DOI: 10.1029/2005gl024348.

5 K. Acker, D. Beysens and D. Möller, Nitrite in dew, fog, cloud and rain water: An indicator for heterogeneous processes on surfaces, *Atmos. Res.*, 2008, **87**, 200–212, DOI: 10.1016/j.atmosres.2007.11.002.

6 D. Luckhaus, Multi-arrangement quantum dynamics in 6D:cis-trans isomerization and 1,3-hydrogen transfer in HONO, *Chem. Phys.*, 2004, **304**, 79–90, DOI: 10.1016/j.chemphys.2004.06.038.

7 H. Meusel, A. Tamm, U. Kuhn, D. M. Wu, A. L. Leifke, S. Fiedler, N. Ruckteschler, P. Yordanova, N. Lang-Yona, M. Pöhlker, J. Lelieveld, T. Hoffmann, U. Pöschl, H. Su, B. Weber and Y. F. Cheng, Emission of nitrous acid from soil and biological soil crusts represents an important source of HONO in the remote atmosphere in Cyprus, *Atmos. Chem. Phys.*, 2018, **18**, 799–813, DOI: 10.5194/acp-18-799-2018.

8 J. Kleffmann, Daytime sources of nitrous acid (HONO) in the atmospheric boundary layer, *ChemPhysChem*, 2007, **8**, 1137–1144, DOI: 10.1002/cphc.200700016.

9 M. Sörgel, E. Regelin, H. Bozem, J. M. Diesch, F. Drewnick, H. Fischer, H. Harder, A. Held, Z. Hosaynali-Beygi, M. Martinez and C. Zetzsch, Quantification of the unknown HONO daytime source and its relation to NO_2, *Atmos. Chem. Phys.*, 2011, **11**, 10433–10447, DOI: 10.5194/acp-11-10433-2011.

10 W. Q. Zhang, S. R. Tong, C. H. Jia, L. L. Wang, B. X. Liu, G. Q. Tang, D. S. Ji, B. Hu, Z. R. Liu, W. R. Li, Z. Wang, Y. Liu, Y. S. Wang and M. F. Ge, Different HONO Sources for Three Layers at the Urban Area of Beijing, *Environ. Sci. Technol.*, 2020, **54**, 12870–12880, DOI: 10.1021/acs.est.0c02146.

11 F. Bao, M. Li, Y. Zhang, C. Chen and J. Zhao, Photochemical Aging of Beijing Urban $PM_{2.5}$: HONO Production, *Environ. Sci. Technol.*, 2018, **52**, 6309–6316, DOI: 10.1021/acs.est.8b00538.

12 D. Xia, X. Zhang, J. Chen, S. Tong, H.-b. Xie, Z. Wang, T. Xu, M. Ge and D. T. Allen, Heterogeneous formation of HONO catalyzed by CO_2, *Environ. Sci. Technol.*, 2021, **55**, 12215–12222, DOI: 10.1021/acs.est.1c02706.

13 Y. L. Liu, W. Nie, Z. Xu, T. Y. Wang, R. X. Wang, Y. Y. Li, L. Wang, X. G. Chi and A. J. Ding, Semi-quantitative understanding of source contribution to nitrous acid (HONO) based on 1 year of continuous observation at the SORPES station in eastern China, *Atmos. Chem. Phys.*, 2019, **19**, 13289–13308, DOI: 10.5194/acp-19-13289-2019.

14 C. Y. Xue, Substantially growing interest in the chemistry of nitrous acid (HONO) in China: current achievements, problems, and future directions, *Environ. Sci. Technol.*, 2022, **56**, 7375–7377, DOI: 10.1021/acs.est.2c02237.

15 E. J. Slater, L. K. Whalley, R. Woodward-Massey, C. X. Ye, J. D. Lee, F. Squires, J. R. Hopkins, R. E. Dunmore, M. Shaw, J. F. Hamilton, A. C. Lewis, L. R. Crilley, L. Kramer, W. Bloss, T. Vu, Y. L. Sun, W. Q. Xu, S. Y. Yue, L. J. Ren, W. J. F. Acton, C. N. Hewitt, X. M. Wang, P. Q. Fu and D. E. Heard, Elevated levels of OH observed in haze events during wintertime in central Beijing, *Atmos. Chem. Phys.*, 2020, **20**, 14847–14871, DOI: 10.5194/acp-20-14847-2020.

16 L. K. Whalley, E. J. Slater, R. Woodward-Massey, C. Ye, J. D. Lee, F. Squires, J. R. Hopkins, R. E. Dunmore, M. Shaw, J. F. Hamilton, A. C. Lewis, A. Mehra, S. D. Worrall, A. Bacak, T. J. Bannan, H. Coe, C. J. Percival, B. Ouyang, R. L. Jones, L. R. Crilley, L. J. Kramer, W. J. Bloss, T. Vu, S. Kotthaus, S. Grimmond, Y. Sun, W. Xu, S. Yue, L. Ren, W. J. F. Acton, C. N. Hewitt, X. Wang, P. Fu and D. E. Heard, Evaluating the sensitivity of radical chemistry and ozone formation to ambient VOCs and NO_x in Beijing, *Atmos. Chem. Phys.*, 2021, **21**, 2125–2147, DOI: 10.5194/acp-21-2125-2021.

17 C. Y. Xue, C. L. Zhang, C. Ye, P. F. Liu, V. Catoire, G. Krysztofiak, H. Chen, Y. G. Ren, X. X. Zhao, J. H. Wang, F. Zhang, C. X. Zhang, J. W. Zhang, J. L. An, T. Wang, J. M. Chen, J. Kleffmann, A. Mellouki and Y. J. Mu, HONO budget and its role in nitrate formation in the rural north China plain, *Environ. Sci. Technol.*, 2020, **54**, 11048–11057, DOI: 10.1021/acs.est.0c01832.

18 X. Fu, T. Wang, L. Zhang, Q. Y. Li, Z. Wang, M. Xia, H. Yun, W. H. Wang, C. Yu, D. L. Yue, Y. Zhou, J. Y. Zheng and R. Han, The significant contribution of HONO to secondary pollutants during a severe winter pollution event in southern China, *Atmos. Chem. Phys.*, 2019, **19**, 1–14, DOI: 10.5194/acp-19-1-2019.

19 H. Xuan, Y. Zhao, Q. Ma, T. Chen, J. Liu, Y. Wang, C. Liu, Y. Wang, Y. Liu, Y. Mu and H. He, Formation mechanisms and atmospheric implications of summertime nitrous acid (HONO) during clean, ozone pollution and double high-level $PM_{2.5}$ and O_3 pollution periods in Beijing, *Sci. Total Environ.*, 2023, **857**, 159538, DOI: 10.1016/j.scitotenv.2022.159538.

20 L. Xu, S. Liu, Y. Tang, X. Han, Y. Wang, D. Fu, Q. Qin and Y. Xu, Long-term dechlorination of polychlorinated biphenyls (PCBs) in Taihu lake sediment microcosms: identification of new pathways, PCB-driven shifts of microbial communities, and insights into dechlorination potential, *Environ. Sci. Technol.*, 2021, **56**, 938–950, DOI: 10.1021/acs.est.1c06057.

21 K. Johnson, J. Xu, A. Yerkeson and M. M. Lu, The catalytic hydro-dechlorination of 2, 4, 4′ trichlorobiphenyl at mild temperatures and atmospheric pressure, *J. Air Waste Manage. Assoc.*, 2024, **74**, 457–463, DOI: 10.1080/10962247.2024.2353643.

22 A. Martínez, Toxicity of persistent organic pollutants: a theoretical study, *J. Mol. Model.*, 2024, **30**, 97, DOI: 10.1007/s00894-024-05890-8.

23 B. C. Kelly, Food web-specific biomagnification of persistent organic pollutants (vol 317, pg 236, 2007), *Science*, 2007, **318**, 44, DOI: 10.1126/science.1144865.

24 K. Lyall, L. A. Croen, A. Sjödin, C. K. Yoshida, O. Zerbo, M. Kharrazi and G. C. Windham, Polychlorinated biphenyl and organochlorine pesticide concentrations in maternal mid-pregnancy serum samples: association with autism spectrum disorder and intellectual disability, *Environ. Health Perspect.*, 2017, **125**, 474–480, DOI: 10.1289/Ehp277.

25 S. Zhang, W. Ouyang, X. Xia, W. Wen, L. Adrian and G. Schüürmann, Mechanistic insight into the Dehalococcoides-mediated reductive dechlorination of polychlorinated biphenyls, *Phys. Chem. Chem. Phys.*, 2023, **25**, 15193–15199, DOI: 10.1039/d3cp01055d.

26 G. Q. Qin, R. Y. Jia, J. T. Xue, L. Chen, Y. Li, W. M. Luo, X. M. Wu, T. F. An and Z. Z. Fang, New perspectives on the risks of hydroxylated polychlorinated biphenyl (OH-PCB) exposure: intestinal flora α-glucosidase inhibition, *Toxics*, 2024, **12**, 237, DOI: 10.3390/toxics12040237.

27 K. C. Jones and P. de Voogt, Persistent organic pollutants (POPs): state of the science, *Environ. Pollut.*, 1999, **100**, 209–221, DOI: 10.1016/s0269-7491(99)00098-6.

28 J. T. Chen and K. B. Li, Research on pollution and treatment of polychlorinated biphenyls in China, *Sci. Tech. Inf.*, 2007, 154–155, DOI: 10.16661/j.cnki.1672-3791.2007.26.020.

29 J. F. Wei, X. Zhao, L. Y. Jing, Q. W. Li and R. Zhang, Polychlorinated biphenyls (PCBs) pollution status, processing methods and research prospects in the environment, *Appl. Chem. Ind.*, 2019, **48**, 1908–1913, DOI: 10.16581/j.cnki.issn1671-3206.2019.08.011.

30 W. Z. Hong, Y. M. Li, L. N. Zhang, J. Bao, P. Wang, C. F. Zhu and Q. H. Zhang, Levels and distribution of polychlorinated biphenyls in the atmosphere of Beijing, *Environ. Chem.*, 2015, **34**, 410–416, DOI: 10.7524/j.issn.0254-6108.2015.03.2014093004.

31 C. Yuan, K. Croft, S. de Nicola, A. P. Davis and B. V. Kjellerup, Treatment of polycyclic aromatic hydrocarbons (PAHs) and polychlorinated biphenyls (PCBs) in stormwater using polishing columns with biochar and granular activated carbon, *Chemosphere*, 2025, **372**, 144107, DOI: 10.1016/j.chemosphere.2025.144107.

32 N. N. Wu, W. M. Cao, R. J. Qu, D. M. Zhou, C. Sun and Z. Y. Wang, Photochemical transformation of decachlorobiphenyl (PCB-209) on the surface of microplastics in aqueous solution, *Chem. Eng. J.*, 2021, **420**, 129813, DOI: 10.1016/j.cej.2021.129813.

33 M. A. J. Harrison, S. Barra, D. Borghesi, D. Vione, C. Arsene and R. Iulian Olariu, Nitrated phenols in the atmosphere: a review, *Atmos. Environ.*, 2005, **39**, 231–248, DOI: 10.1016/J.ATMOSENV.2004.09.044.

34 F. Elisei, G. Favaro and A. Romani, A laser flash photolysis study of di-pyridyl ketones, *Chem. Phys.*, 1990, **144**, 107–115, DOI: 10.1016/0301-0104(90)80076-A.

35 Y. Hu, J. Ma, M. Zhu, Y. Zhao, S. Peng and C. Zhu, Photochemical oxidation of o-dichlorobenzene in aqueous solution by hydroxyl radicals from nitrous acid, *J. Photochem. Photobiol., A*, 2021, **420**, 113503, DOI: 10.1016/j.jphotochem.2021.113503.

36 J. Z. Ma, C. Z. Zhu, J. Lu, T. Wang, S. H. Hu and T. H. Chen, Photochemical reaction between biphenyl and N(III) in the atmospheric aqueous phase, *Chemosphere*, 2017, **167**, 462–468, DOI: 10.1016/j.chemosphere.2016.10.010.

37 T. Arakaki, T. Miyake, T. Hirakawa and H. Sakugawa, pH dependent photoformation of hydroxyl radical and absorbance of aqueous-phase N(III) (HNO_2 and NO_2^-), *Environ. Sci. Technol.*, 1999, **33**, 2561–2565, DOI: 10.1021/es980762i.

38 C. Anastasio and L. Chu, Photochemistry of nitrous acid (HONO) and nitrous acidium Ion (H_2ONO^+) in aqueous solution and ice, *Environ. Sci. Technol.*, 2009, **43**, 1108–1114, DOI: 10.1021/es802579a.

39 B. Priyadharshini, S. Verma, A. Chatterjee, S. K. Sharma and T. K. Mandal, Chemical characterization of fine atmospheric particles of water-soluble ions and carbonaceous species in a tropical urban atmosphere over the eastern indo-gangetic plain, *Aerosol Air Qual. Res.*, 2019, **19**, 129–147, DOI: 10.4209/aaqr.2017.12.0606.

40 G. V. Buxton, C. L. Greenstock, W. P. Helman and A. B. Ross, Critical review of rate constants for reactions of hydrated electrons, hydrogen atoms and hydroxyl radicals (OH/O) in aqueous solution, *J. Phys. Chem. Ref. Data*, 1988, **17**, 513–886, DOI: 10.1063/1.555805.

41 G. Merga, B. S. M. Rao, H. Mohan and J. P. Mittal, Reactions of OH and SO_4.bul.- with some halobenzenes and halotoluenes: A radiation chemical study, *J. Phys. Chem.*, 1994, **98**, 9518–9164, DOI: 10.1021/j100088a012.

42 Z. Liao, M. Zeng and L. Wang, Atmospheric oxidation mechansim of polychlorinated biphenyls (PCBs) initiated by OH radicals, *Chemosphere*, 2020, **240**, 124756, DOI: 10.1016/j.chemosphere.2019.124756.

43 K. Sehested and E. J. Hart, Formation and decay of the biphenyl cation radical in aqueous acidic solution, *J. Phys. Chem.*, 2002, **79**, 1639–1642, DOI: 10.1021/j100583a005.

44 C. Z. Zhu, B. Ouyang, H. J. Fang, W. B. Dong, Z. J. Zheng, Q. X. Zhao and H. Q. Hou, Study on the cross-reaction mechanism of aqueous benzene with nitrous acid in dilute solutions by transient absorption spectrum technique, *Acta Chim. Sin.*, 2004, **62**, 1115–1122.

45 L. Huang, R. Zhang, D. Gu, P. Li, W. Dong and H. Hou, Mechanism study on the reactions between biphenyl and HNO_2 initiated by 355 nm irradiation in aqueous phase, *Sci. China, Ser. B: Chem.*, 2007, **50**, 700–706, DOI: 10.1007/s11426-007-0089-6.

46 G. Hizal, Q. Q. Zhu, C. H. Fischer, P. M. Fritz and W. Schnabel, On the photolysis of phthalic acid dialkyl esters: a product analysis study, *J. Photochem. Photobiol., A*, 1993, **72**, 147–152, DOI: 10.1016/1010-6030(93)85021-y.

47 J. Z. Ma, C. Z. Zhu, J. Lu, Y. Lei, J. Z. Wang and T. H. Chen, Photochemical reaction between triclosan and nitrous acid in the atmospheric aqueous environment, *Atmos. Environ.*, 2017, **157**, 38–48, DOI: 10.1016/j.atmosenv.2017.03.011.

48 Z. H. Liao, M. Zeng and L. M. Wang, Atmospheric oxidation mechansim of polychlorinated biphenyls (PCBs) initiated by OH radicals, *Chemosphere*, 2020, **240**, 124756, DOI: 10.1016/j.chemosphere.2019.124756.

49 W. Q. Cao, N. N. Wu, S. N. Zhang, Y. M. Qi, R. X. Guo, Z. Y. Wang and R. J. Qu, Photodegradation of polychlorinated biphenyls in water/nitrogen-doped silica and air/nitrogen-doped silica systems: Kinetics, mechanism and quantitative structure activity relationship (QSAR) analysis, *Sci. Total Environ.*, 2024, **924**, 171586, DOI: 10.1016/j.scitotenv.2024.171586.

50 M. Fischer and P. Warneck, Photodecomposition of nitrite and undissociated nitrous acid in aqueous solution, *J. Phys. Chem.*, 1996, **100**, 18749–18756, DOI: 10.1021/jp961692.

51 Y. N. Lee and X. Zhou, Aqueous reaction kinetics of ozone and dimethylsulfide and its atmospheric implications, *J. Geophys. Res.: Atmos.*, 2012, **99**, 3597–3605, DOI: 10.1029/93jd02919.

52 J. Shi, W. Bi, S. Li, W. Dong and J. Chen, Reaction mechanism of 4-chlorobiphenyl and the NO_3 radical: an experimental and theoretical study, *J. Phys. Chem. A*, 2017, **121**, 3461–3468, DOI: 10.1021/acs.jpca.6b08626.

53 Y. Q. Yan, Z. S. Wei, X. G. Duan, M. C. Long, R. Spinney, D. D. Dionysiou, R. Y. Xiao and P. J. J. Alvarez, Merits and limitations of radical vs. nonradical pathways in persulfate-based advanced oxidation processes, *Environ. Sci. Technol.*, 2023, **57**, 12153–12179, DOI: 10.1021/acs.est.3c05153.

54 D. E. Heard and M. J. Pilling, Measurement of OH and HO_2 in the troposphere, *Chem. Rev.*, 2003, **103**, 5163–5198, DOI: 10.1021/cr020522s.

55 H. Herrmann, Kinetics of aqueous phase reactions relevant for atmospheric chemistry, *Chem. Rev.*, 2003, **103**, 4691–4716, DOI: 10.1021/cr020658q.